

1
2
3
4
5 **Cyclopalladated and cycloplatinated benzophenone imines: Antitumor,**
6 **antibacterial and antioxidant activities, DNA interaction and cathepsin B**
7 **inhibition**
8
9

10 Joan Albert ^{a,f,*}, Lucía D'Andrea ^a, Jaume Granell ^{a,f}, Pepita Pla-Vilanova ^a,
11 Josefina Quirante ^{b,**}, Muhammad Kaleem Khosa ^c, Carme Calvis ^d, Ramon
12 Messeguer ^d, Josefa Badía ^{e,f}, Laura Baldomà ^{e,f}, Mercè Font-Bardia ^{g,h}, Teresa
13 Calvet ^g
14
15

16 ^a Departament de Química Inorgànica, Facultat de Química, Universitat de Barcelona, Martí i
17 Franquès 1–11, 08028 Barcelona, Spain

18 ^b Laboratori de Química Orgànica, Facultat de Farmàcia, Universitat de Barcelona, Av. Joan XXIII
19 s/n, 08028 Barcelona, Spain

20 ^c Department of Chemistry, Government College University, Faisalabad, Pakistan

21 ^d Biomed Division LEITAT Technological Center, Parc Científic, Edifici Hèlix, Baldori Reixach 15–
22 21, 08028 Barcelona, Spain

23 ^e Departament de Bioquímica i Biologia Molecular, Facultat de Farmàcia, Universitat de Barcelona,
24 Av. Joan XXIII s/n, 08028 Barcelona, Spain

25 ^f Institut de Biomedicina (IBUB), Universitat de Barcelona, Barcelona, Spain

26 ^g Departament de Cristallografia, Mineralogia i Dipòsits Minerals, Universitat de Barcelona, Martí i
27 Franquès s/n, 08028 Barcelona, Spain

28 ^h Unitat de Difracció de RX, Centre Científic i Tecnològic de la Universitat de Barcelona, Solé i
29 Sabarís 1–3, 08028 Barcelona, Spain
30

31
32
33
34 * Correspondence to: J. Albert, Departament de Química Inorgànica, Facultat de Química, Universitat
35 de Barcelona, Martí i Franquès 1–11, 08028 Barcelona, Spain. Tel.: +34 93 4039131.

36 ** Corresponding author. Tel.: +34 93 4035849.

37 E-mail addresses: joan.albert@qi.ub.es (J. Albert), quirantese@ub.edu (J. Quirante).
38

39 **Keywords:** Cyclometalated Palladium Platinum Anticancer DNA Metalloproteases
40

41 **ABSTRACT**

42

43 The antitumor, antibacterial and antioxidant activity, DNA interaction and cathepsin B inhibition of
44 cyclo-orthopalladated and -platinated compounds $[\text{Pd}(\text{C},\text{N})]_2(\mu\text{-X})_2$ [$\text{X} = \text{OAc}$ (1), $\text{X} = \text{Cl}$ (2)] and
45 $\text{trans-N,P-[M}(\text{C},\text{N}) \text{X}(\text{PPh}_3)]$ [$\text{M} = \text{Pd}$, $\text{X} = \text{OAc}$ (3), $\text{M} = \text{Pd}$, $\text{X} = \text{Cl}$ (4), $\text{M} = \text{Pt}$, $\text{X} = \text{Cl}$ (5)] are
46 discussed [(C,N)= cyclo-orthometallated benzophenone imine]. The cytotoxicity of compound 5 has
47 been evaluated towards human breast (MDA-MB-231 and MCF-7) and colon (HCT-116) cancer cell
48 lines and that of compounds 1–4 towards the HCT-116 human colon cancer cell line. These
49 cytotoxicities have been compared with those previously reported for compounds 1–4 towards MDA-
50 MB-231 and MCF-7 cancer cell lines. Compound 3 and 4 were approximately four times more active
51 than cisplatin against the MDA-MB-231 and MCF-7 cancer cell lines, and compound 5, was
52 approximately four times more potent than cisplatin against the HCT-116 cancer cell line. The
53 antibacterial activity of compounds 1–5 was in between the ranges of activity of the commercial
54 antibiotic compounds cefixime and roxithromycin. Complexes 1–2 and 4–5 presented also antioxidant
55 activity. Compounds 1–5 alter the DNA tertiary structure in a similar way to cisplatin, but at higher
56 concentration, and do not present a high efficiency as cathepsin B inhibitors. Compound 5 has not been
57 previously described, and its preparation, characterization, and X-ray crystal structure are reported.

58

59

60

61

62 1. Introduction

63

64 The application of cyclometalated compounds in medicine and bioimaging is a subject of growing
65 interest [1–3]. In this field, our research group has published some studies on the in vitro antitumor
66 activity of cyclopalladated and cycloplatinated compounds [4–7]. The number of studies related to the
67 anticancer activity of cyclopalladated and cycloplatinated compounds is quite significant [8,9] but very
68 little is known about their other chemotherapeutic activities. Antiparasitic activity has been reported for
69 a few cyclopalladated and cycloplatinated compounds [5,10–12]. In addition, in a few cases the
70 antibacterial activity of cyclopalladated compounds has also been studied [13–16]. Cycloaurated
71 compounds have also been explored for their antibacterial, antifungal, antiviral and antiparasitic
72 activities [12,17,18].

73 On the other hand, in recent years, it has become increasingly evident that several cytotoxic metallodrugs
74 exert their biological and pharmacological actions through DNA-independent mechanisms.
75 Accordingly, it is important to explore alternative mechanisms and biological targets for
76 anticancer metallodrugs [19]. Cathepsin B is a cysteine metalloprotease highly upregulated in a wide
77 variety of cancers by mechanisms ranging from gene amplification to post-transcriptional modification.
78 The exact role of cathepsin B in solid tumors has yet to be defined, but it has been proposed to participate
79 in metastasis, angiogenesis, and tumor progression [20,21]. Recently, compounds based on palladium,
80 platinum, ruthenium, rhenium, gold and tellurium were shown to be effective inhibitors of cathepsin B
81 [12,20–31]. In addition, an excellent correlation between cathepsin B inhibition and cytotoxicity for
82 some dinuclear biphosphane palladacycles [22] and mononuclear platinacycles containing a fluorinated
83 phosphane [28] has been reported. Therefore within this work, we intended to study the capability of
84 the cyclopalladated and cycloplatinated benzophenone imines 1–5 given in Scheme 1 to act as cytotoxic
85 agents, by direct damage on DNA, or/and by inhibiting alternative targets such as cathepsin B, which is
86 overexpressed in many cancer cell lines.

87 In a precedent paper [32], we reported the antitumor activity of the cyclopalladated benzophenone
88 imines 1–4 depicted in Scheme 1 against the MDA-MB-231 and MCF-7 human breast cancer cell lines
89 and studied their interaction towards DNA by the DNA migration electrophoretic technique. Following
90 this study, here we report: a) the antitumor activity of compounds 1–4 towards the HCT-116 human
91 colon cancer cell line and that of the cycloplatinated compound 5 towards MDA-MB-231 and MCF-7
92 breast and HCT-116 colon human cancer cell lines, b) the antibacterial activity of compounds 1–5, c)
93 the antioxidant activity of compounds 1–5, expressed as their % of DPPH free radical scavenging, d)
94 the interaction of compound 5 with DNA by the DNA migration agarose gel electrophoretic assay, and
95 e) the cathepsin B inhibition test for compounds 1–5.

96

97

98

99 2. Experimental

100

101 2.1. Chemistry: instruments and reagents

102

103 Elemental analyses of C, H and N were performed with an Eager 1108 microanalyzer. Infrared spectra
104 were recorded on a Nicolet Impact-400 spectrophotometer using pressed disks of dispersed samples of
105 the compounds in KBr. ^1H NMR (at 400 MHz), ^{13}C - $\{^1\text{H}\}$ (at 101 MHz), ^{195}Pt - $\{^1\text{H}\}$ (at 86 MHz),
106 and ^{31}P - $\{^1\text{H}\}$ (at 162 MHz) NMR spectra were recorded in CDCl_3 at 298 K. Chemical shifts are
107 reported in δ values (ppm) relative to SiMe_4 ($\delta=0.00$ ppm) for ^1H NMR, to the residual solvent peak
108 for ^{13}C - $\{^1\text{H}\}$ ($\delta = 77.00$ ppm), to a solution of $\text{K}_2[\text{PtCl}_4]$ in D_2O ($\delta = -1617.00$ ppm) as an external
109 reference for ^{195}Pt - $\{^1\text{H}\}$ NMR, and relative to an external solution of trimethylphosphite in deuterated
110 acetone ($\delta = 140.18$ ppm relative to 85% orthophosphoric acid) for ^{31}P - $\{^1\text{H}\}$ NMR. Coupling constants
111 are given in Hz, and multiplicity (splitting) is expressed as s (singlet), d (doublet), m (multiplet), and br
112 (broad signal). Low resolution ESI (+) mass spectrawere acquired on an LC/MSD-TOF instrument,
113 utilizing a mixture of $\text{CH}_3\text{CN}:\text{H}_2\text{O}$ (1:1, v/v) as the eluent. Dry methanol (HPLC grade),
114 dichloromethane, hexanes, ethyl acetate, and diethyl ether were used as received. Sodium acetate was
115 oven-dried at 60°C , prior to use. The complex $\text{cis-}[\text{PtCl}_2(\text{DMSO})_2]$ was prepared following a literature
116 method [33]. Compounds 1–4 were prepared as previously reported [32]. ESI and LC/MSD-TOF refer
117 to Electrospray Ionization and Liquid Chromatography/Mass Selective Detector — Time Of Flight,
118 respectively.

119

120 2.2. Preparation of mixture A

121

122 $\text{Cis-}[\text{PtCl}_2(\text{DMSO})_2]$ (301 mg, 0.71 mmol) and sodium acetate (61 mg, 0.74 mmol) were brought into
123 a Schlenk flask and evacuated for 10 min, and finally flushed with nitrogen. To this, dry methanol (50
124 mL) was added and the reaction mixture was warmed until complete dissolution of the sample. An
125 excess of benzophenone imine (150 μL , 162 mg, 0.89 mmol) was next added to the yellow solution, and
126 the resulting mixture was refluxed for 1 day. After this time, dichloromethane (approx. 15 mL) was added
127 to the red solution to induce precipitation of the sodium acetate. The suspension was filtered through a
128 pad of celite (5.0 cm \times 2.0 cm) and washed through with further dichloromethane until the washings went
129 colorless. Evaporation of the solvent resulted in the formation of a resin, to which hexanes (ca. 15 mL)
130 were added. The mixture was energetically stirred for 1–2 days, during which time intense scratching
131 on the vessel surface was required to help promoting precipitation. The beige solid was collected by
132 filtration and air-dried (305 mg). ^1H NMR characterization in CDCl_3 revealed that the major
133 components of this solid are $\text{trans-N,L-}[\text{Pt}(\text{C,N})\text{Cl}(\text{DMSO})]$ (A1) and trans-N,L-
134 $[\text{Pt}(\text{C,N})\text{Cl}(\text{Ph}_2\text{C}=\text{NH})]$ (A2) in a 3:1 molar ratio. ^1H NMR (400MHz, CDCl_3 , 298 K) (selected data):
135 A1: 8.83 (br s, 1 H, NH), 8.27 (d, $3J_{\text{HH}} = 7.6$, $3J_{\text{PtH}} = 48.0$, 1H, H2), 3.56 (s, $3J_{\text{PtH}} = 21.4$, 6H, CH3);
136 A2: 10.0 (br s, 1H, NH), 8.92 (br s, 1H, NH), 8.29 (d, $3J_{\text{HH}} = 7.2$, partially overlapped with H2 of A1,
137 1H, H2). MSESI (+) ($\text{CH}_3\text{CN}:\text{H}_2\text{O}$, (1:1)), m/z: A1: 494.1 (calcd. 494.1) $[\text{M} - \text{Cl} + \text{CH}_3\text{CN}]^+$, 453.1
138 (calcd. 453.1) $[\text{M} - \text{Cl}]^+$; A2: 597.2 (calcd. 597.2) $[\text{M} - \text{Cl} + \text{CH}_3\text{CN}]^+$, 556.1 (calcd. 556.1) $[\text{M} - \text{Cl}]^+$.

139

140

141

142

143 2.3. Preparation of compound 5

144

145 The mixture A (297 mg) was dissolved in acetone (50 mL) giving an orange solution, which was
 146 subsequently treated with triphenylphosphane (160 mg, 0.61 mmol) at room temperature. After 2 h and
 147 30 min of stirring, the resulting mixture was concentrated under vacuum. Addition of diethyl ether
 148 (approx. 10 mL) produced the formation of a yellow precipitate, which was filtered and air-dried (290
 149 mg). An additional crop was obtained from the ether mother liquor, which was concentrated to dryness
 150 and afterwards vigorously stirred in hexanes (ca. 25 mL) for one day. The yellow solid formed was
 151 filtered off and dried in air (40 mg). Both crops were combined, dissolved in ethyl acetate, and subjected
 152 to column chromatography (SiO₂, 3.0 cm × 30 cm) using a 100:60 hexanes:ethyl acetate mixture as
 153 eluent. The eluted band led to the required product after solvent removal and addition of hexanes (ca.
 154 10mL). The yellow solid obtained was recovered by filtration and air-dried (128 mg, 27% yield, relative
 155 to the starting *cis*-[PtCl₂(DMSO)₂]). Yellow crystals of 5 suitable for X-ray analysis were grown at
 156 room temperature from a dichloromethane solution layered by hexanes in a 1:1 volume ratio. IR
 157 (selected data), ν (cm⁻¹): 3315 (NH st), 1583 (C = N st), 1096 (q, X-sensitive PPh₃). ¹H NMR (400
 158 MHz, CDCl₃, 298 K): 9.34 (br s, 1 H, NH), 7.80–7.75 (m, 6 H, *o*-PPh₃), 7.61–7.52 (m, 5 H, H₈ + H₉
 159 + H₁₀), 7.47–7.37 (m, 9 H, *p*-PPh₃ + *m*-PPh₃), 7.16 (d, 1 H, 3J_{HH} = 7.8, H₅), 6.92–6.88 (m, 1 H, H₄),
 160 6.74–6.58 (m, 2 H, H₂ + H₃). ¹³C-{¹H} NMR (101 MHz, CDCl₃, 298 K): 189.1 (d, 3J_CP = 2.6, C₇ =
 161 NH), 145.9 (d, 3J_CP = 1.5, C₆), 145.3 (d, 2J_CP = 6.7, C₁), 137.8 (d, 3J_CP = 5.9, C₂), 135.4 (d, 2J_CP =
 162 11.3, *o*-CPPh₃), 134.9 (d, 4J_CP = 5.0, C₈), 132.7 (d, 4J_CP = 2.0, C₃), 131.3 (s, C₅), 131.2 (s, C₁₁),
 163 130.8 (d, 4J_CP = 2.5, *p*-CPPh₃), 130.1 (d, 1J_CP = 60.2, *i*-CPPh₃), 129.0 (s, C₁₀), 128.0 (d, 3J_CP = 11.0,
 164 *m*-CPPh₃), 127.8 (s, C₉), 122.6 (s, C₄). ³¹P-{¹H} NMR (162 MHz, CDCl₃, 298 K): 22.64 (s, 1J_PT =
 165 4068). ¹⁹⁵Pt-{¹H} NMR (86 MHz, CDCl₃, 298 K): -4206.6 (d, 1J_PT = 4109). MS-ESI (+)
 166 (CH₃CN:H₂O, (1:1)), *m/z*: 1309.2 (calcd. 1309.2) [2M - Cl]⁺, 678.2 (calcd. 678.2) [M - Cl +
 167 CH₃CN]⁺, 637.1 (calcd. 637.1) [M - Cl]⁺. Anal. Calcd. for C₃₁H₂₅ClN₂Pt: C 55.32%, H 3.74%, N
 168 2.08%. Found: C 55.16%, H 3.81%, N 1.97%.

169

170 2.4. X-ray crystal structure determination of compound 5

171

172 A yellow prism-like specimen of compound 5 (C₃₁H₂₅ClN₂Pt), approximate dimensions 0.208 mm ×
 173 0.249 mm × 0.554 mm, was used for the X-ray crystallographic analysis. The X-ray intensity data were
 174 measured on a D8 Venture system equipped with a multilayer monochromator and a Mo microfocus (λ
 175 = 0.71073 Å). A total of 2848 frames were collected. The total exposure time was 7.91 h. The frames
 176 were integrated with the Bruker SAINT software package [34] using a narrow-frame algorithm. The
 177 integration of the data using a triclinic unit cell yielded a total of 91349 reflections to a maximum θ
 178 angle of 36.42° (0.60 Å resolution), of which 24376 were independent (average redundancy 3.747,
 179 completeness = 99.7%, R_{int} = 4.35%) and 23182 (95.10%) were greater than 2 σ (F₂). The final cell
 180 constants of *a* = 9.709(1) Å, *b* = 10.255(1) Å, *c* = 14.027(2) Å, α = 74.231(3)°, β = 72.613(4)°, γ =
 181 77.491(4)°, volume = 1268.6(3) Å³, are based upon the refinement of the XYZ-centroids of 195
 182 reflections above 20 σ (I) with 5.583° *b* 2 θ *b* 58.11°. Data were corrected for absorption effects using the
 183 multi-scan method (SADABS). The ratio of minimum to maximum apparent transmission was 0.727.
 184 The structure was solved and refined using the Bruker SHELXTL Software Package [35], with *Z* = 2
 185 for the formula unit, C₃₁H₂₅ClN₂Pt. The final anisotropic full-matrix least-squares refinement on F₂
 186 with 316 variables converged at R₁ = 1.67%, for the observed data and wR₂ = 4.29% for all data. The
 187 goodness-of-fit was 1.116. The largest peak in the final difference electron density synthesis was 1.100
 188 e⁻/Å³ and the largest hole was -1.695 e⁻/Å³ with an RMS (Root Mean Square) deviation of 0.122
 189 e⁻/Å³. On the basis of the final model, the calculated density was 1.762 g/cm³ and F(000), 656 e⁻.

190 2.5. Cell culture

191

192 Breast cancer [MCF-7 (Michigan Cancer Foundation-7) and MBAMD-231 (M. D. Anderson-Metastatic
193 Breast-231)] and colon cancer [HCT-116 (Human Colon Tumor-116)] cells were grown as a monolayer
194 culture in minimum essential medium (DMEM with L-glutamine, without glucose and without sodium
195 pyruvate) in the presence of 10% heat-inactivated fetal calf serum, 10 mM D-glucose and 0.1%
196 streptomycin/penicillin, in standard culture conditions (humidified air with 5% CO₂ at 37 °C).

197

198 2.6. Cell viability assay

199

200 A stock solution (50 mM) of each compound was prepared in high purity DMSO. Then, serial dilutions
201 were made with DMSO (1:1) and finally a 1:500 dilution of the diluted solutions of compounds on cell
202 media was prepared. In this way DMSO concentration in cell media was always the same. The assay
203 was performed as described by Givens et al. [36]. HCT-116, MDA-MB-231 and MCF-7 cells were
204 plated at 5000 cells/well, respectively, in 100 mL media in tissue culture 96-well plates (Cultek). After
205 24 h, media was replaced by 100 mL/well of drug serial dilutions. Control wells did not contain
206 compounds 1–5. Each point concentration was run in triplicate. Reagent blanks, containing media and
207 colorimetric reagent without cells were run on each plate. Blank values were subtracted from test values
208 and were routinely 5–10% of the control values. Plates were incubated 72 h. Hexosaminidase activity
209 was measured according to the following protocol. The media were removed and cells were washed
210 once with PBS (Phosphate Buffered Saline). Then, 60 mL of substrate solution (p-nitrophenol-N-acetyl-
211 β -D-glucosamide 7.5 mM, sodium citrate 0.1 M at pH 5.0, and 0.25% Triton X-100) was added to each
212 well and incubated at 37 °C for 1–2 h. After this incubation time, a bright yellow appeared. Then, the
213 plates were developed by adding 90 mL of developer solution (glycine 50 mM, pH 10.4; EDTA 5 mM)
214 and the absorbance was recorded at 410 nm.

215

216 2.7. Antibacterial activity

217

218 Test compounds (1–5) were screened to determine their antibacterial activity against six bacterial
219 strains; three gram positive *Staphylococcus aureus* (ATCC 6538), *Micrococcus luteus* (ATCC 10240)
220 and *Bacillus subtilis* (ATCC 6633) and three gram negative *Escherichia coli* (ATCC 15224),
221 *Enterobacter aerogenes* (ATCC 13048) and *Bordetella bronchiseptica* (ATCC 4617) by using “Disc
222 diffusion method” [37–39]. The organisms were cultured in nutrient broth at 37 °C for 24 h. One percent
223 broth culture containing approx. 10⁶ colony-forming units (CFU/mL) of test strain were added to
224 nutrient agar medium at 45 °C and poured into sterile petri plates. The medium was allowed to solidify.
225 Five microliters of the test compound (40 mg/mL in DMSO) was poured on 4-mm sterile paper disks
226 and placed on nutrient agar plates respectively. In each plate DMSO served as negative control and
227 standard antibacterial drugs roxithromycin (1 mg/mL) and cefixime (1 mg/mL) served as a positive
228 control. Triplicate plates of each bacterial strain were prepared. The plates were incubated at 37 °C for
229 24 h. The antibacterial activity was determined by measuring the diameter of zones showing complete
230 inhibition (mm).

231

232

233 2.8. DPPH (1,1-diphenyl-2-picrylhydrazyl) free radical scavenging assay

234

235 The scavenging activity of DPPH free radicals of compounds 1–5 was determined according to the
 236 method reported earlier with minor modifications [40,41]. A stock solution (5 mg/mL) of test solution
 237 was prepared in DMSO. Serial dilutions were carried out to obtain concentrations of 5, 10, 20, 40, 100,
 238 200 µg/mL. 15 µL of each test sample or DMSO in case of negative control was mixed with 2985 µL of
 239 0.1 mM methanolic solution of DPPH in glass vials so that the final volume was 3 mL. The vials were
 240 capped and reaction mixture was incubated for 30 min at 37 °C in dark. After incubation the change in
 241 colour (from deep-violet to light-yellow) of DPPH solution was measured by taking absorbance of
 242 reaction mixtures at 517 nm on a PDA (photo diode array) spectrophotometer (Agilent 8453). Mixture
 243 of 2985 µL of methanol and 15 µL of DMSO was used as a blank for spectrophotometric measurements.
 244 Each concentration was assayed in triplicate. Ascorbic acid was used as a reference standard and
 245 dissolve in distilled water to make the stock solution with the same concentration (5 mg/mL). Control
 246 was prepared containing the same volume without any test solution and reference ascorbic acid. The %
 247 scavenging of the DPPH free radical was calculated by using the following formula.

248

$$249 \quad \% \text{scavenging activity} = \frac{\text{absorbance of control} - \text{absorbance of test sample}}{\text{absorbance of control}} \times 100$$

250

251 2.9. DNA migration studies

252

253 A stock solution (10 mM) of each compound was prepared in high purity DMSO. Then, serial dilutions
 254 were made in MilliQ water (1:1). Plasmid pBluescript SK + (Stratagene) was obtained using QIAGEN
 255 plasmid midi kit as described by the manufacturer. Interaction of drugs with pBluescript SK + plasmid
 256 DNA was analyzed by agarose gel electrophoresis following a modification of the method described by
 257 Abdullah et al. [42]. Plasmid DNA aliquots (40 µg/mL) were incubated in TE buffer (10 mM Tris-HCl,
 258 1 mM EDTA, pH 7.5) with different concentrations of compounds 1–5 ranging from 0 µM to 200 µM
 259 at 37 °C for 24 h. Final DMSO concentration in the reactions was always lower than 1%. For comparison,
 260 cisplatin and ethidium bromide were used as reference controls. Aliquots of 20 µL of the incubated
 261 solutions of compounds containing 0.8 µg of DNA were subjected to 1% agarose gel electrophoresis in
 262 TAE buffer (40 mM Tris-acetate, 2 mM EDTA, pH 8.0). The gel was stained in TAE buffer containing
 263 ethidium bromide (0.5 mg/mL) and visualized and photographed under UV light.

264

265 2.10. Cathepsin B inhibition assay

266

267 Aldrich (C6286). The colorimetric cathepsin B assay was performed as described by Casini et al. [27],
 268 with few modifications. Briefly, the reaction mixture contained 100 mM sodium phosphate (pH 6.0), 1
 269 mM EDTA and 200 µM sodium N-carbobenzoxy-L-lysine p-nitrophenyl ester as substrate. To have the
 270 enzyme catalytically active before each experiment the active site of the cysteine was reduced by
 271 treatment with dithiothreitol (DTT). For this purpose, 5 mM DTT was added to cathepsin B sample,
 272 before dilution, and incubated 1 h at 30 °C. To test the inhibitory effect of the compounds 1–5 on
 273 cathepsin B, activity measurements were performed in triplicate using fixed concentrations of enzyme
 274 (500 nM) and substrate (200 µM). Compounds were used at concentrations ranging from 10 to 100 µM.
 275 Previous to the addition of substrate, cathepsin B was incubated with the different compounds at 25 °C

276 for 24 h. The cysteine proteinase inhibitor E-64 was used as a positive control of cathepsin B inhibition.
277 Complete inhibition was achieved at 10 μ M concentration of E-64. Activity was measured over 1.5 min.
278 at 326 nm on a UV-1603 spectrophotometer (Shimadzu).

279

280

281 3. Results and discussion

282

283 3.1. Synthesis of compounds 1–5

284

285 Scheme 1 shows the methods of preparation of compounds 1–5 and the numbering of the hydrogen and
286 carbon atoms of the benzophenone imine for the discussion that follows.

287 Cyclopalladated benzophenone imines 1–4 were prepared according to the methods recently reported by
288 our research group [32]. Mixture A was prepared by a modification of the reported procedure for the
289 cycloplatination of benzophenone imine [43,44]. Cis-[PtCl₂(DMSO)₂] and NaOAc in molar ratio 1:1
290 were treated with an excess of benzophenone imine in dry methanol under nitrogen and at reflux for 24
291 h. In these conditions, we were able to isolate mixture A in a moderate amount, which contained as
292 major components the cycloplatinated compounds [Pt(C,N)Cl(L)] A1 (L= DMSO) and A2 (L=
293 benzophenone imine). Other minor compounds present in mixture A could not be characterized. Mixture
294 A was studied by ¹H NMR and ESI mass spectrometry. Analysis of the integrals of the ¹H NMR
295 indicates that compounds A1 and A2 were the major components of mixture A and that the molar ratio
296 between them was A1/A2 ≈ 3/1. Compound 5 of formula trans-N,P-[Pt(C,N)Cl(PPh₃)] was prepared by
297 reaction between mixture A and PPh₃ via a substitution reaction of the L ligand in compounds A1 and
298 A2 for the PPh₃ ligand. Compound 5 was obtained in 27% yield relative to the initial cis-
299 [PtCl₂(DMSO)₂] and was fully characterized by elemental analysis, IR, NMR and mass spectrometry.
300 In addition, its crystal structure was determined by X-ray diffraction.

301 In the IR spectrum, compound 5 presented the N–H and C–N stretchings and the q X sensitive band of
302 the coordinated PPh₃ molecule at 3315, 1583 and 1096 cm⁻¹, respectively [32]. In the ESI mass
303 spectrometry, compound 5 produced intense signals for the cations [M – Cl + CH₃CN]⁺ and [M – Cl]⁺,
304 in accordance with the labile nature of Pt(II)\Cl σ bond and the coordinative nature of the molecules of
305 acetonitrile, which was used as a solvent in this technique [45]. The most interesting features of the ¹H
306 NMR spectrum of compound 5 were: i) the lack of the signal due to the H₁ proton, which demonstrated
307 its ortho-metallated nature, ii) the chemical shift of its NH proton (9.34 ppm) relative to free
308 benzophenone imine (8.40 ppm), which was consistent with the coordination of the iminic nitrogen to
309 the platinum(II) center, and iii) the chemical shift of the H₂–H₅ protons of the ortho-platinated phenyl
310 ring in the interval between 7.16 and 6.58 ppm, which was consistent with the trans-N,P configuration
311 of compound 5 [32,45–48]. Protons H₂–H₅ present these low chemical shifts because they are located
312 in the shielding zone of the PPh₃ aromatic rings of compound 5 [32,35–38]. The κC1, κN chelate
313 coordination mode of the benzophenone imine in compound 5 could also be determined by ¹³C–{¹H}
314 NMR since, in this experiment, the ¹³C (C1 and C7) atoms produced doublets due to the coupling of
315 these ¹³C nuclei with the ³¹P nucleus [45].

316 ³¹P–{¹H} NMR of compound 5 produced a singlet at 22.64 ppm with the expected satellites for ¹⁹⁵Pt
317 with a coupling constant between ³¹P and ¹⁹⁵Pt of 4068 Hz, and the ¹⁹⁵Pt–{¹H} NMR produced a
318 doublet at –4206.6 ppm with a coupling constant between ³¹P and ¹⁹⁵Pt of 4068 Hz. These chemical
319 shifts for ³¹P and ¹⁹⁵Pt and coupling constant between ³¹P and ¹⁹⁵Pt were quite similar to those
320 previously reported for compounds of formula trans-N,P-[Pt(C,N)Cl(PPh₃)], being (C,N) an ortho-
321 cycloplatinated benzalimine or cycloplatinated ferrocenylimine with the iminic bond included in the
322 metalacycle [49,50].

323

324

325

326 3.2. Molecular crystal structure of compound 5

327

328 Suitable crystals for the X-ray molecular crystal structure determination of compound 5 were grown by
329 slow evaporation of a solution of compound 5 in CH₂Cl₂/hexane in a volume ratio 1:1. Compound 5
330 crystallized in the triclinic space group P-1 with Z = 2. Fig. 1 shows the X-ray molecular structure of 5
331 and gives selected distances and bond angles. The molecular structure determined by X-ray diffraction
332 confirms the proposed structure for compound 5. The benzophenone imine is coordinated in a chelate
333 form to the platinum(II) through the N1 and C13 atoms, and a chlorido ligand and the phosphorus atom
334 of the triphenylphosphane ligand complete the square-planar coordination sphere of the platinum(II)
335 center. The triphenylphosphane ligand is in trans position to the iminic nitrogen atom, in accordance
336 with the trans-N,P configuration proposed for compound 5 by NMR. Distances and angles around the
337 platinum(II) center are between the normal intervals [50], being the C(13)–Pt(1)–N(1) [79.80(5)°] and
338 C(13)–Pt(1)–Cl(1) [167.74(4)°] those that deviated most from the ideal angles for a square planar-
339 geometry (90 and 180°). The atoms coordinated to the platinum(II) center (Cl1, P1, C13 and N1) were
340 almost in a plane and the metalacycle (Pt1, C13, C8, C1 and N1) was practically planar. The N1 atom
341 (–0.068 Å) for the coordination plane and the C1 (–0.045 Å) atom for the metalacycle were those that
342 were deviated most from their respective planes. The coordination plane (Cl1, P1, C13 and N1) and the
343 ortho-metalated phenyl ring (C13, C12, C11, C10, C9 and C8) were almost coplanar, being the angle
344 between these two planes 4.84°, and the angle between the planes of the non-metalated phenyl ring (C7,
345 C6, C5, C4, C3 and C2) and the metalacycle was 45.81°.

346

347 3.3. Stability and behavior in solution of compounds 1–5

348

349 Compounds 1–5 were stable for long periods of time in contact with air, both in the solid state and in
350 CDCl₃ solution. These compounds were also soluble in DMSO. In this solvent, the dinuclear compounds
351 1 and 2 should be converted by a splitting reaction into the mononuclear compounds I of formula trans-
352 N,S-[Pd(C,N)(S-DMSO)X] (X = OAc or Cl) [45,51]. In DMSO as solvent, the exchange of PPh₃ for
353 DMSO in compounds 3–5 does not seem likely because the favorable thermodynamic reaction is the
354 inverse of this reaction [52]. In addition, in the biological media, complexes I, 3, 4 and 5 could be
355 converted into the ionic aqua complexes [Pd(C,N)(H₂O)₂]X (X = OAc, Cl) (compounds II) and trans-
356 N,P-[M(C,N)(PPh₃)(H₂O)]X (M = Pd, X = OAc or Cl and M = Pt, X = Cl) (compounds III) by
357 substitution of the chlorido and DMSO ligands of compounds I and the chlorido ligands of compounds
358 3–5 for water molecules, respectively. Therefore, we propose that the species responsible for the
359 biological activities studied below are the ionic aqua complexes II and III commented above [32].

360

361

362

363 3.4. Antiproliferative studies

364

365 Compound 5 was evaluated in vitro for inhibition of cell proliferation against MDA-MB-231 and MCF-
366 7 human breast cancer cell lines, using cisplatin as a positive control. All the investigated compounds
367 (1–5) were also evaluated against the cisplatin resistant HCT-116 human colon cancer cell line using
368 cisplatin as a reference. The effects of the assayed palladacycles (1–4) and platinacycle (5) on the growth
369 of the selected cell lines were assessed after 72 h and the IC₅₀ values of compounds 1–5 resulting from

370 an average of two experiments are listed in Table 1. The cytotoxicity of compounds 1–4 towards the
371 human breast MDA-MB-231 and MCF-7 cancer cell lines has been previously reported and their IC₅₀
372 values are included in Table 1 for a comparative purpose [32].

373 The in vitro data for the antiproliferative effect of 1–5 (Table 1) reveals that the different complexes
374 inhibit cell proliferation in varying degrees depending on the cell line assayed. Most of the compounds
375 exhibited a remarkable antiproliferative activity with IC₅₀ values lower than those of cisplatin in the
376 three cell lines assayed. Platinacycle 5 showed the highest cytotoxicity towards the HCT-116 cancer
377 cells, while palladacycles 3 and 4 were the most potent against the MDA-MB-231 and MCF-7 cancer
378 cells. Interestingly, platinacycle 5 was found to inhibit cell growth proliferation of the HCT-116 colon
379 cell line at a concentration approximately four times lower than cisplatin. In addition, we reported
380 recently [32] that compounds 3 and 4 were approximately four times more potent than cisplatin against
381 the MDA-MB231 and MCF-7 human breast cancer cell lines. It should also be noted that free
382 benzophenone imine was not active against the studied tumor cell lines.

383

384 3.5. Antibacterial activity

385

386 Resistance to chemotherapeutic agents is a common drawback of both anticancer and anti-infectious
387 treatments. Hence, there is a need for new class of chemotherapeutic drugs in treating cancer cells and
388 pathogenic microorganisms. On the other hand, patients with neoplastic disorders who are subjected to
389 chemotherapeutic treatment are susceptible to microbial infections due to the subsequent drop of
390 immunity. Therefore, the search of single drugs, which would possess dual anticancer and antibacterial
391 activity, might be advantageous both therapeutically and cost-effectively.

392 Based on the previous assumptions, compounds 1–5 were screened for their antibacterial activity against
393 three Gram-positive (*S. aureus*, *M. luteus* and *B. subtilis*) and three Gram-negative (*E. coli*, *E. aerogenes*
394 and *B. bronchi*) bacterial strains by the disk diffusion method. The commercial antibiotics cefixime
395 (third generation cephalosporin) and roxithromycin (semi-synthetic macrolide) were used as positive
396 controls. The results of antibacterial activities in the form of MIC are summarized in Table 2.

397 Compounds 1–5 showed varying degrees of antibacterial activity with MIC values in the interval 0.18–
398 0.34 μ M against the studied Gram-positive and Gram-negative bacterial strains (see Table 2). The
399 antibacterial activity of compounds 1–5 is in between the ranges of activity of the commercial antibiotic
400 cefixime and roxithromycin. It is interesting to note that all of the compounds showed antibacterial
401 activity against the Gram-negative *E. aerogenes* strain and that compounds 1–5 were more active against
402 Gram-negative strains than Gram-positive strains. This latter result is interesting since Gram-negative
403 bacterial resistance is a burgeoning problem in intensive care units [53]. The best antibacterial activity
404 was provided by platinacycle 5, which exhibit MIC values lower than that of roxithromycin against *E.*
405 *coli* (Gram-negative), *E. aerogenes* (Gram-negative) and *B. subtilis* (Gram-positive).

406

407 3.6. Antioxidant activity

408

409 The potential preventive anticancer effects of antioxidants, found in high concentrations in many
410 phytochemicals, have become a major focus of research in recent years. These agents block free radical
411 formation as an important mediator of their anticancer effects. Despite accumulating evidence to suggest
412 an important role of antioxidants in cancer prevention, there has been much controversy over their
413 potential therapeutic applications [54–58]. Very recently, antioxidant phytochemicals have found a

414 chemopreventive effect in platins based chemotherapies [59–61]. Furthermore, the biological activity
415 of specific platinum derivatives, such as the platinum nitrosyl complexes are presumable due in part to
416 the antioxidant properties of the nitrosyl pharmacophore [62]. Therefore we were interested in
417 evaluating the antioxidant capability of the studied cyclometalated complexes.

418 The antioxidant activity of compounds 1–5 was evaluated by their DPPH (1,1-diphenyl-2-
419 picrylhydrazyl) free radical scavenging activity. The DPPH monoradical presents a strong absorption at
420 517 nm, which gives place to its violet colour. DPPH colour changes to light yellow when it accepts an
421 electron or a hydrogen atom from an antioxidant compound. This discoloration can be quantitatively
422 measured from the change in absorbance. Free radical scavenging activity of antioxidant compounds is
423 concentration-dependent. Then, the radical scavenging activity increases as concentration of the
424 antioxidant compound increases, and a low IC₅₀ value reflects a high antioxidant activity [40,41].

425 DPPH free radical scavenging activities of complexes 1–5 were assayed at six concentrations (200, 100,
426 40, 20, 10 and 5 µg/mL) and the results are summarized in Table 3. Ascorbic acid was used as a positive
427 control. As expected, DPPH free radical scavenging activity of tested compounds was concentration
428 dependent. Hence higher radical scavenging was observed at higher concentrations, i.e. 200 µg/mL.
429 DPPH scavenging analysis showed that compounds 1–2 and 4–5 are good scavengers of DPPH by
430 scavenging 69–81% of the radicals at 200 µg/mL. This scavenging activity is very close to that of
431 ascorbic acid (87%) at the same final concentration (200 µg/mL). IC₅₀ values for complexes 1–2 and
432 4–5 for the DPPH free radical scavenging were in the interval between 0.12 and 0.14 µM. It should be
433 noted that the mononuclear palladium(II) compound 3, with the terminal acetate ligand did not present
434 any significant antioxidant activity. At present, we cannot give a mechanism for the DPPH scavenging
435 activity of these kinds of compounds.

436

437

438

439 3.7. DNA migration studies

440

441 The interaction of compound 5 with DNA was studied by its ability to modify the electrophoretic
442 mobility of the supercoiled closed circular (ccc) and the open circular (oc) forms of pBluescript SK +
443 plasmid DNA (Fig. 2). The ccc form usually moves faster due to its compact structure. For comparison
444 purposes cisplatin and ethidium bromide were included in the experiment. When the test compounds
445 were incubated with plasmid DNA at 37 °C, they coordinated to DNA molecule, which in some
446 extent was cleaved into fragments, and the brightness of the band diminished in gel.

447 In spite of the high antiproliferative activity of compound 5, it was less efficient than cisplatin for
448 removing the supercoils from pBluescript SK+ plasmid DNA, suggesting that the unwinding of the DNA
449 is not the key factor responsible of their cytotoxicity (Fig. 2) [32].

450 An unwinding experiment was performed with increasing concentration of compound 5 ranging from 0
451 to 200 µM and 40 µg/mL of pBluescript (Fig. 2). In the presence of platinum cycle 5, the rate of migration
452 of the supercoiled band (ccc) decreased and tended to approach that of the nicked relaxed band (oc) at
453 concentration 25 µM. At higher concentration, an unwinding of negative to positive supercoiled DNA
454 was displayed in the electrophoretogram (Fig. 3, compound 5, lanes 6–8). The same effect was observed
455 for cisplatin (Fig. 2, cisplatin, lanes 3 and 5).

456 Compounds 1–4 were less efficient than compound 5 in removing the supercoils of DNA [32]. Up to 50
457 µM, only a slight decrease in the rate of migration of the supercoiled closed circular form was observed

458 for the dinuclear compound 2. At 100 μM , palladium compounds 1–4 greatly altered the mobility of the
459 plasmid DNA. The unwinding of negative to positive supercoiled DNA was also observed for the Pd(II)
460 complexes 1–4 but at 200 μM .

461 Thus, on the basis of the alteration of the electrophoretic mobility of pBluescript plasmid DNA, it is
462 hypothesized that compounds 1–5 alter the DNA tertiary structure by the same mechanism than
463 cisplatin, but at higher concentrations.

464

465 3.8. Cathepsin B inhibition

466

467 The cytotoxicity of some dinuclear biphosphane palladacycles (Fig. 3, compounds X) [22] and
468 mononuclear platinacycles with a fluorinated phosphane ligand (Fig. 3, compounds Y) [28] has been
469 related to their cathepsin B inhibitory properties. In addition, several mononuclear cyclopalladated and
470 cycloaurated complexes (Fig. 3, compounds Z) with antiparasitic activity were also excellent inhibitors
471 of cathepsin B [12]. Considering the interaction of cyclopalladated compounds with cathepsin B, it is
472 worthy of mention that their inhibition properties are very dependent on their structure and their IC50
473 values vary in a very wide range [22].

474 Based on the precedent results, we were interested in testing the efficiency of compounds 1–5 as
475 inhibitors of cathepsin B. Fig. 4 shows that compounds 1–5 inhibit cathepsin B in a dose dependent
476 manner but none of compounds 1–5 had a high efficiency as cathepsin B inhibitor. Among them, only
477 compound 4 inhibited more than 50% the enzyme activity at 100 μM concentration. Platinacycle 5
478 presented a cathepsin B inhibition efficiency lower than that of palladacycles 1–4. This result should be
479 related with the great reactivity of the palladium(II) centers in compounds 1–4 in relation to the
480 platinum(II) center in compound 5 [8].

481 The low activity of compounds 1–5 for the inhibition of cathepsin B could be related with an insufficient
482 targeting of compounds 1–5 for the active site of cathepsin B or with a lack of reactivity of their metal
483 center for the active site of cathepsin B [63]. It should be noted that a hydrogen bond between the N–H
484 function of compounds 1–5 and the anionic X ligand trans to the metalated carbon atom could render
485 the metal centers of compounds 1–5 less reactive to substitution reactions than expected.

486

487 4. Conclusions

488 .

489 The chemotherapeutic properties of cyclopalladated and cycloplatinated benzophenone imines studied
490 in this work and in a previous one [32] show that these kinds of compounds have potential as anticancer
491 agents, and they also present antibacterial and antioxidant activity. The best results for the three activities
492 reported here (cytotoxicity versus HC-T116 colon cancer cells, antibacterial activity
493 against Gram-negative microorganisms and antioxidant properties) were found for the newly prepared
494 and characterized cycloplatinated complex 5.

495 Cyclopalladated compounds 3–4 showed a remarkable antiproliferative activity against MDA-MB-231
496 and MCF-7 breast human cancer cell lines and produced an approximately four-fold increase in potency
497 with regard to cisplatin [32]. In addition, platinumacycle 5 also showed an approximately four-fold increase
498 in potency in relation to cisplatin in human HCT-116 colon cancer cells [this work]. These results
499 uncover a greater selectivity of platinumacycle 5 against the HCT-116 colon cancer cell line, whereas
500 palladacycles 3 and 4 exhibit a greater selectivity for MDA-MB231 and MCF-7 breast cancer cells.

501 Interestingly, compounds 1–5 also presented antibacterial and antioxidant activity. Compounds 1–5
502 exhibited greater activity against Gram-negative than against Gram-positive bacterial strains, with MIC
503 values between those of the commercial antibiotic cefixime and roxithromycin. The platinum compound
504 5 turned out to be more potent in antibacterial activity than palladium compounds 1–4. Complexes 1–2
505 and 4–5 presented also antioxidant activity with IC₅₀ values in the interval 0.12–0.14 μM . The nature
506 of the metal center (Pt vs. Pd) does not discriminate upon the radical scavenging activity of the assayed
507 cyclometalated complexes.

508 With regard to plausible target biomolecules for compounds 1–5, these metalacycles altered the DNA
509 tertiary structure in a similar way as the standard reference cisplatin but at higher concentrations. Thus,
510 retardation of the DNA mobility was observed at 25 μM for compound 5 and at 100 μM for compounds
511 1–4. On the other hand, compounds 1–5 did not present a high activity for the inhibition of cathepsin B,
512 being palladacycles 1–4 more active than platinumacycle 5 versus the inhibition of cathepsin B. Then, there
513 is no correlation between the cytotoxic activity of the studied compounds 1–5 and their inhibitory
514 activity on this cysteine protease. These results suggest that these classes of compounds (cyclopalladated
515 and platinated benzophenone imines), both with good cytotoxic activity, operate via a different
516 pharmacological mechanism in which DNA and cathepsin B are not the primary targets.

517 Work is in progress in our research group with the aims of firstly finding out a plausible primary target
518 biomolecule for these compounds, then to functionalize compounds 1–5 in an adequate form in order to
519 increase their potency as anticancer agents, and also to study the mechanism through that these
520 compounds scavenges the DPPH radicals.

521

522 **Acknowledgements**

523

524 We are grateful to the Ministerio de Ciencia y Tecnología (Grant CTQ2009-11501), the AGAUR
525 (Generalitat de Catalunya, Grant 2009-SGR-1111) and Higher Education Commission of Pakistan
526 (Grant No. 20-1434) for the financial support.

527

528 **References**

529

- 530 [1] N. Cutillas, G.S. Yellol, C. de Haro, C. Vicente, V. Rodríguez, J. Ruiz, *Coord. Chem. Rev.* 257
531 (2013) 2784–2797.
- 532 [2] Q. Zhao, C. Huang, F. Li, *Chem. Soc. Rev.* 40 (2011) 2508–2524.
- 533 [3] V. Fernández-Moreira, F.L. Thorp-Greenwood, M.P. Coogan, *Chem. Commun.* 46 (2010) 186–
534 202.
- 535 [4] J. Albert, R. Bosque, M. Crespo, J. Granell, C. López, R. Cortés, A. Gonzalez, J. Quirante, C.
536 Calvis, R. Messeguer, L. Baldomà, J. Badia, M. Cascante, *Bioorg. Med. Chem.* 21 (2013) 4210–
537 4217.
- 538 [5] D. Talancón, C. López, M. Font-Bardia, T. Calvet, J. Quirante, C. Calvis, R. Messeguer, R.
539 Cortés, M. Cascante, L. Baldomà, J. Badia, *J. Inorg. Biochem.* 118 (2013) 1–12.
- 540 [6] R. Cortés, M. Crespo, L. Davin, R. Martín, J. Quirante, D. Ruiz, R. Messeguer, C. Calvis, L.
541 Baldomà, J. Badia, M. Font-Bardia, T. Calvet, M. Cascante, *Eur. J. Med. Chem.* 54 (2012) 557–
542 566.
- 543 [7] J. Quirante, D. Ruiz, A. Gonzalez, C. López, M. Cascante, R. Cortés, R. Messeguer, C. Calvis, L.
544 Baldomà, A. Pascual, Y. Guérardel, B. Pradines, M. Font-Bardia, T. Calvet, C. Biot, *J. Inorg.*
545 *Biochem.* 105 (2011) 1720–1728.
- 546 [8] A.C.F. Caires, *Anti Cancer Agents Med. Chem.* 7 (2007) 484–491.
- 547 [9] A. Gómez Quiroga, C. Navarro Ranninger, *Coord. Chem. Rev.* 248 (2004) 119–133.
- 548 [10] M. Adams, C. de Kock, P.J. Smith, K. Chibale, G.S. Smith, *J. Organomet. Chem.* 736 (2013)
549 19–26.
- 550 [11] P. Chellan, K.M. Land, A. Shokar, A. Au, S.H. An, C.M. Clavel, P.J. Dyson, C. de Kock, P.J.
551 Smith, K. Chibale, G.S. Smith, *Organometallics* 31 (2012) 5791–5799.
- 552 [12] S.P. Fricker, R.M. Mosi, B.R. Cameron, I. Baird, Y. Zhu, V. Anastassov, J. Cox, P.S. Doyle, E.
553 Hansell, G. Lau, J. Langille, M. Olsen, L. Qin, R. Skerlj, R.S.Y. Wong, Z. Santucci, J.H.
554 McKerrow, *J. Inorg. Biochem.* 102 (2008) 1839–1845.
- 555 [13] E. Budzisz, R. Bobka, A. Hauss, J.N. Roedel, S. Wirth, I.P. Lorenz, B. Rozalska, M.
556 Więckowska-Szakiel, U. Krajewskad, M. Rozalskid, *Dalton Trans.* 41 (2012) 5925–5933.
- 557 [14] H.J. Lee, S.H. Lee, H.C. Kim, Y.-E. Lee, S. Park, *J. Organomet. Chem.* 717 (2012) 164–171.
- 558 [15] A.C. Moro, A.C. Urbaczek, E.T. De Almeida, F.R. Pavan, C.Q.F. Leite, A.V.G. Netto, A.E.
559 Mauro, *J. Coord. Chem.* 65 (2012) 1434–1442.
- 560 [16] A.C. Moro, A.E. Mauro, A.V.G. Netto, S.R. Ananias, M.B. Quilles, I.Z. Carlos, F.R. Pavan,
561 C.Q.F. Leite, M. Hörner, *Eur. J. Med. Chem.* 44 (2009) 4611–4615.
- 562 [17] M.B. Dinger, W. Henderson, *J. Organomet. Chem.* 560 (1998) 233–243.
- 563 [18] R.V. Parish, J. Mack, L. Hargreaves, J.P. Wright, R.G. Buckley, A.M. Elsome, S.P. Fricker,
564 B.R.C. Theobald, *J. Chem. Soc. Dalton Trans.* (1996) 69–74.
- 565 [19] N.P.E. Barry, P.J. Sadler, *Chem. Commun.* 49 (2013) 5106–5131.
- 566 [20] M.M. Mohamed, B.F. Sloane, *Nat. Rev. Cancer* 6 (2006) 764–775.

- 567 [21] S.P. Fricker, *Metalomics* 2 (2010) 366–377.
- 568 [22] J. Spencer, A. Casini, O. Zava, R.P. Rathnam, S.K. Velhanda, M. Pfeffer, S.K. Callear, M.B.
569 Hursthouse, P.J. Dyson, *Dalton Trans.* (2009) 10731–10735.
- 570 [23] J. Spencer, R.P. Rathnam, M. Motukuri, A.K. Kotha, S.C.W. Richardson, A. Hazrati, J.A.
571 Hartley, L. Louise, M.B. Hursthouse, *Dalton Trans.* (2009) 4299–4303.
- 572 [24] S.S. Gunatilleke, A.M. Barrios, *J. Inorg. Biochem.* 102 (2008) 555–563.
- 573 [25] R. Mosi, I.R. Baird, J. Cox, V. Anastassov, B. Cameron, R.T. Skerlj, S.P. Fricker, *J. Med. Chem.*
574 49 (2006) 5262–5272.
- 575 [26] T.S. Abondanza, C.R. Oliveira, C.M.V. Barbosa, F.E.G. Pereira, R.L.O.R. Cunha, A.C.F.
576 Caires, C. Bincoletto, *Food Chem. Toxicol.* 46 (2008) 2540–2545.
- 577 [27] A. Casini, C. Gabbiani, F. Sorrentino, M.P. Rigobello, A. Bindoli, T.J. Geldbach, A. Marrone, N.
578 Re, C.G. Hartinger, P.J. Dyson, L. Messori, *J. Med. Chem.* 51 (2008) 6773–6781.
- 579 [28] N. Cutillas, A. Martínez, G.S. Yellol, V. Rodríguez, A. Zamora, M. Pedreño, A. Donaire, Ch.
580 Janiak, J. Ruiz, *Inorg. Chem.* 52 (2013) 13529–13535.
- 581 [29] C. Bincoletto, I.L.S. Tersariol, C.R. Oliveira, S. Dreher, D.M. Fausto, M.A. Soufen, F.D.
582 Nascimento, A.C.F. Caires, *Bioorg. Med. Chem.* 13 (2005) 3047–3055.
- 583 [30] S.S. Gunatilleke, A.M. Barrios, *J. Med. Chem.* 49 (2006) 3933–3937.
- 584 [31] R.L.O.R. Cunha, M.E. Urano, J.R. Chagas, P.C. Almeida, C. Bincoletto, I.L.S. Tersariol, J.V.
585 Comasseto, *Bioorg. Med. Chem. Lett.* 15 (2005) 755–760.
- 586 [32] J. Albert, S. García, J. Granell, A. Llorca, M.V. Lovelle, V. Moreno, A. Presa, L. Rodríguez, J.
587 Quirante, C. Calvis, R. Messeguer, J. Badía, L. Baldomà, *J. Organomet. Chem.* 724 (2013) 289–
588 296.
- 589 [33] V.Y. Kukushkin, A.J.L. Pombeiro, C.M.P. Ferreira, L.I. Elding, *Inorg. Synth.* 33 (2002) 189–
590 196.
- 591 [34] SAINT Bruker, Bruker AXS Inc., Madison, Wisconsin, USA, 2007.
- 592 [35] G.M. Sheldrick, *Acta Crystallogr. A* 64 (2008) 112–122.
- 593 [36] K.T. Givens, S. Kitada, A.K. Chen, J. Rothschilder, D.A. Lee, *Investig. Ophthalmol. Vis. Sci.*
594 31 (1990) 1856.
- 595 [37] A. Felten, B. Grandry, P.H. Lagrange, I. Casin, *J. Clin. Microbiol.* 40 (2002) 2766–2771.
- 596 [38] M. Jamil, I.U. Haq, B. Mirza, M. Qayyum, *Ann. Clin. Microbiol. Antimicrob.* 11 (2012) 11.
- 597 [39] S. Arikan, V. Paetznick, J.H. Rex, *Antimicrob. Agents Chemother.* 46 (2002) 3084–3087.
- 598 [40] G. Cao, E. Sofic, R.L. Prior, *J. Agric. Food Chem.* 44 (1996) 3426–3431.
- 599 [41] H. Nawaz, Z. Akhter, S. Yasmeen, H.M. Siddiqi, B. Mirza, A. Rifat, *J. Organomet. Chem.* 694
600 (2009) 2198–2203.
- 601 [42] A. Abdullah, F. Huq, A. Chowdhury, H. Tayyem, P. Beale, K. Fisher, *BMC Chem. Biol.* 6
602 (2006), <http://dx.doi.org/10.1186/1472-6769-6-3>.
- 603 [43] Y.Y. Scaffidi-Domianello, A.A. Nazarov, M. Haukka, M. Galanski, B.K. Keppler, J. Schneider,
604 P. Du, R. Eisenberg, V.Y. Kukushkin, *Inorg. Chem.* 46 (2007) 4469–4482.

- 605 [44] S.U. Pandya, K.C.Moss, M.R. Bryce, A.S. Batsanov, M.A. Fox, V. Jankus, H.A. Al Attar, A.P.
606 Monkman, *Eur. J. Inorg. Chem.* (2010) 1963–1972.
- 607 [45] J. Albert, R. Bosque, L. D'Andrea, J. Granell, M. Font-Bardia, T. Calvet, *Eur. J. Inorg. Chem.*
608 (2011) 3617–3631.
- 609 [46] J. Albert, L. D'Andrea, J. Granell, R. Tavera, M. Font-Bardia, X. Solans, *J. Organomet. Chem.*
610 692 (2007) 3070–3080.
- 611 [47] J. Albert, J.M. Cadena, A. González, J. Granell, X. Solans, M. Font-Bardia, *Chem. Eur. J.* 12
612 (2006) 887–894.
- 613 [48] J. Albert, J. Granell, J. Sales, M. Font-Bardia, X. Solans, *Organometallics* 14 (1995) 1393–1404.
- 614 [49] X. Riera, A. Caubet, C. López, V. Moreno, X. Solans, M. Font-Bardia, *Organometallics* 19
615 (2000) 1384–1390.
- 616 [50] A. Capapé, M. Crespo, J. Granell, M. Font-Bardia, X. Solans, *J. Organomet. Chem.* 690 (2005)
617 4309–4318.
- 618 [51] J.L. García-Ruano, I. López-Solera, J.R. Masaguer, M.A. Monge, C. Navarro-Ranninger, J.H.
619 Rodríguez, *J. Organomet. Chem.* 476 (1994) 111–120.
- 620 [52] R. Martín, M. Crespo, M. Font-Bardia, T. Calvet, *Polyhedron* 28 (2009) 1369–1373.
- 621 [53] A.F. Shorr, *Crit. Care Med.* 37 (2009) 1463–1469.
- 622 [54] R. Nath, S. Roy, B. De, M.D. Choudhury, *Int. J. Pharm. Pharm. Sci.* 5 (Suppl. 2) (2013) 63–69.
- 623 [55] R. Wilken, M.S. Veena, M.B. Wang, E.S. Srivatsan, *Mol. Cancer* 10 (2011) 12.
- 624 [56] J.H. Lee, T.O. Khor, L. Shu, Z.Y. Su, F. Fuentes, A.N. Tony Kong, *Pharmacol. Ther.* 137 (2013)
625 153–171.
- 626 [57] F. Tosetti, D.M. Noonan, A. Albin, *Int. J. Cancer* 125 (2009) 1997–2003.
- 627 [58] S. Nair, W. Li, A.N. Tony Kong, *Acta Pharmacol. Sin.* 28 (2007) 459–472.
- 628 [59] M.S. Al Moundhri, S. Al-Salam, A. Al Mahrouqee, S. Beegam, B.H. Ali, *J. Med. Toxicol.* 9
629 (2013) 25–33.
- 630 [60] M.U. Nessa, P. Beale, C. Chan, J.Q. Yu, F. Huq, *Anticancer Res.* 32 (2012) 4843–4850.
- 631 [61] P. Ferroni, D. Della-Morte, R. Palmirotta, M. McClendon, G. Testa, P. Abete, F. Rengo, T.
632 Rundek, F. Guadagni, M. Roselli, *Rejuvenation Res.* 14 (2011) 293–308.
- 633 [62] V.D. Sen, V.D. Sen, A.A. Terent'ev, N.P. Konovalova, *Russ. Chem. Bull.* 60 (2011) 1342–1352.
- 634 [63] S. van Zutphen, M. Kraus, C. Driessen, G.A. van der Marel, H.S. Overkleeft, J. Reedijk, *J. Inorg.*
635 *Biochem.* 99 (2005) 1384–1389.

636

637 **Legends to figures**

638

639 **Scheme 1.** i) Pd(OAc)₂ (stoichiometric), HOAc, 60 °C, 24 h; ii) LiCl (excess), acetone, r.t., 2 h; iii)
640 PPh₃ (stoichiometric), acetone, r.t., 2 h.; iv) cis-[PtCl₂(DMSO)₂], NaOAc (stoichiometric),
641 benzophenone imine (excess), methanol, reflux, 24 h, under N₂.

642

643 **Figure 1.** Crystal structure of compound 5. Hydrogen atoms have been omitted for clarity. Selected
644 bond distances (Å) and angles (°): Pt(1)–C(13) = 2.0110(12), Pt(1)–N(1) = 2.0485(10), Pt(1)–P(1) =
645 2.2347(4), Pt(1)–Cl(1) = 2.3622(4), N(1)–C(1) = 1.3000(16), C(1)–C(8) = 1.4586(17), C(8)–C(13) =
646 1.4279(17), C(13)–Pt(1)–N(1) = 79.80(5), C(13)–Pt(1)–P(1) = 96.66(4), N(1)–Pt(1)–P(1) = 173.76(3),
647 C(13)–Pt(1)–Cl(1) = 167.74(4), N(1)–Pt(1)–Cl(1) = 88.09(3), P(1)–Pt(1)–Cl(1) = 95.584(14), C(8)–
648 C(13)–Pt(1) = 113.06(8), C(13)–C(8)–C(1) = 115.17(11), N(1)–C(1)–C(8) = 114.14(10).

649

650 **Figure 2.** Interaction of pBluescript SK+ plasmidDNA (0.8 µg) with increasing concentrations of
651 compound 5, cisplatin and ethidiumbromide. Lane 1: DNA only. Lane 2: 2.5 µM. Lane 3: 5 µM. Lane
652 4: 10 µM. Lane 5: 25 µM. Lane 6: 50 µM. Lane 7: 100 µM. Lane 8: 200 µM. ccc=supercoiled closed
653 circular DNA. oc = open circular DNA.

654

655 **Figure 3.** Structural formula of the compounds under discussion for the cathepsin B inhibition.
656 Compounds X: Dinuclear biphosphane palladacycles [reference 22]. Compounds Y: Mononuclear
657 platinumacycles with a fluorinated phosphane [reference 28]. Compounds Z: Mononuclear cyclopalladated
658 and cycloautared compounds [reference 12].

659

660 **Figure 4.** Effect of compounds 1–5 on cathepsin B activity. The enzyme was preincubated for 24 h with
661 10 µM (blue bars), 50 µM (brown bars) or 100 µM (green bars) of each compound. The activity is given
662 as a percentage of the enzyme activity determined in the absence of the test compound. Data are shown
663 as the mean values of the experiment performed in triplicate with the corresponding standard deviation.

664

665

666

667 **Table 1** IC₅₀ (μM) (50% inhibitory concentration) cytotoxicity for benzophenone imine, compounds
 668 1–5 and cisplatin. Data are shown as the mean values of two experiments performed in triplicate with
 669 the corresponding standard deviation.

Test compound	IC ₅₀ (μM)		
	Cancer cell line		
	MDA-MB-231	MCF-7	HCT-116
Benzophenone imine	>100	>100	>100
1	15.0 ± 1.2 ^a	14.0 ± 4.2 ^a	33 ± 3
2	13 ± 1 ^a	11.0 ± 1.5 ^a	20.0 ± 0.7
3	1.1 ± 0.3 ^a	4.0 ± 0.5 ^a	18 ± 2
4	1.1 ± 0.1 ^a	4.1 ± 0.9 ^a	20 ± 5
5	5.0 ± 1.2	13.4 ± 1.5	11.0 ± 0.6
Cisplatin ^b	6.5 ± 2.4	19.0 ± 4.5	40.0 ± 4.4

^a Data previously reported [32].

^b Cis-[PtCl₂(NH₃)₂] is taken as reference compound.

670

671

672

673 **Table 2** Antibacterial activity of compounds 1–5. *S. aureus*: Staphylococcus aureus. *M. luteus*:
 674 Micrococcus luteus. *B. subtilis*: Bacillus subtilis. *E. coli*: Escherichia coli. *E. aerogenes*: Enterobacter
 675 aerogenes. *B. bronchi*: Bordetella bronchiseptica. Triplicate plates of each bacterial strain were prepared.
 676

Test compound (MW) ^b	MIC ^a [$\mu\text{g} \times \text{ml}^{-1}$ (μM)]					
	Bacterial strain					
	<i>S. aureus</i> ^c	<i>M. luteus</i> ^c	<i>B. subtilis</i> ^c	<i>E. coli</i> ^d	<i>E. aerogenes</i> ^d	<i>B. bronchi</i> ^d
1 (691.38)	- ^e	-	-	-	150 ± 2 (0.22)	150 ± 1 (0.22)
2 (644.20)	-	200 ± 3 (0.31)	-	200 ± 2 (0.31)	150 ± 2 (0.23)	-
3 (607.97)	-	-	-	-	150.0 ± 2.5 (0.25)	150.0 ± 1.5 (0.25)
4 (584.38)	-	-	200 ± 2 (0.34)	-	200 ± 1 (0.34)	-
5 (673.04)	125 ± 1 (0.18)	>200	180 ± 3 (0.27)	170 ± 1 (0.25)	160 ± 1 (0.24)	140.0 ± 0.5 (0.21)
cefixime (453.45)	20.0 ± 0.5 (0.04)	70 ± 1 (0.15)	50 ± 2 (0.11)	50 ± 1 (0.11)	80.0 ± 0.5 (0.18)	60 ± 1 (0.13)
roxitromycin (837.047)	150 ± 3 (0.18)	700 ± 3 (0.84)	600 ± 1 (0.72)	600 ± 2 (0.72)	500 ± 2 (0.60)	70 ± 2 (0.08)

^a MIC = minimum inhibitory concentration that will inhibit the visible growth of a microorganism after 24 h of incubation.

^b MW = molecular weight.

^c Gram-positive.

^d Gram-negative.

^e - = No activity.

677

678

679

680 **Table 3** Antioxidant activity of compounds 1–5 expressed as the % of DPPH free radical scavenging.
 681 Each concentration for the test compounds (200, 100, 40, 20, 10 and 5 µg/mL) was assayed in triplicate.

Test compound (MW) ^c	% scavenging ± SD ^a						IC ₅₀ ^b µg/mL (µM)
	Concentration µg/mL (test compound)						
	200	100	40	20	10	5	
1 (691.38)	74 ± 1	54 ± 2	27.0 ± 0.3	15 ± 1	8.0 ± 0.5	0	87 ± 1 (0.13)
2 (644.20)	69 ± 2	52 ± 1	34 ± 1	22.0 ± 0.5	12 ± 1	5 ± 1	90.0 ± 0.5 (0.14)
3 (607.97)	46 ± 1	37.0 ± 0.5	22.0 ± 0.5	16.0 ± 0.5	3.0 ± 0.5	0	>200
4 (584.38)	72 ± 2	56 ± 2	38 ± 2	21 ± 1	14 ± 1	9 ± 2	74 ± 1 (0.13)
5 (673.04)	81 ± 3	57 ± 0.5	33 ± 1	24.0 ± 0.5	16 ± 2	1 ± 1	81 ± 1 (0.12)
Asc. ac. ^d (176.12)	87.0 ± 0.5	84 ± 1	80.0 ± 0.3	70.0 ± 0.5	56 ± 1	35 ± 1	8.8 ± 0.5 (0.05)

^a SD = standard deviation.

^b IC₅₀ = 50% inhibitory concentration.

^c MW = molecular weight.

^d Asc. ac. = ascorbic acid.

682

683

684

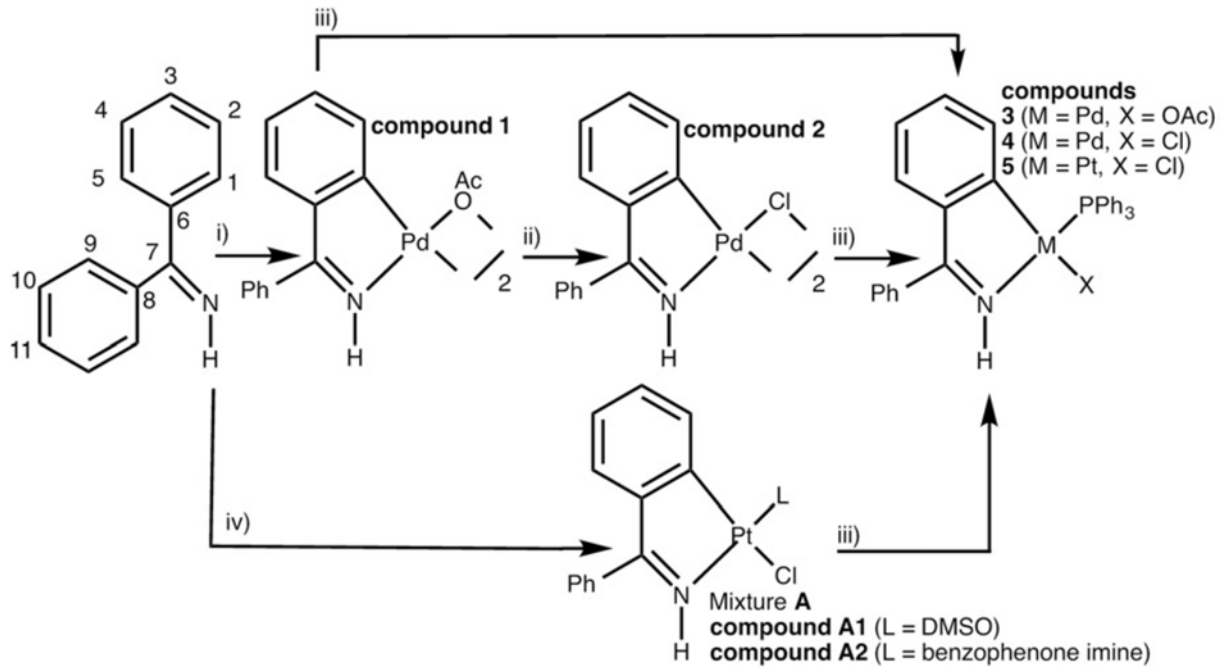
685

686

Scheme 1

687

688



689

690

691

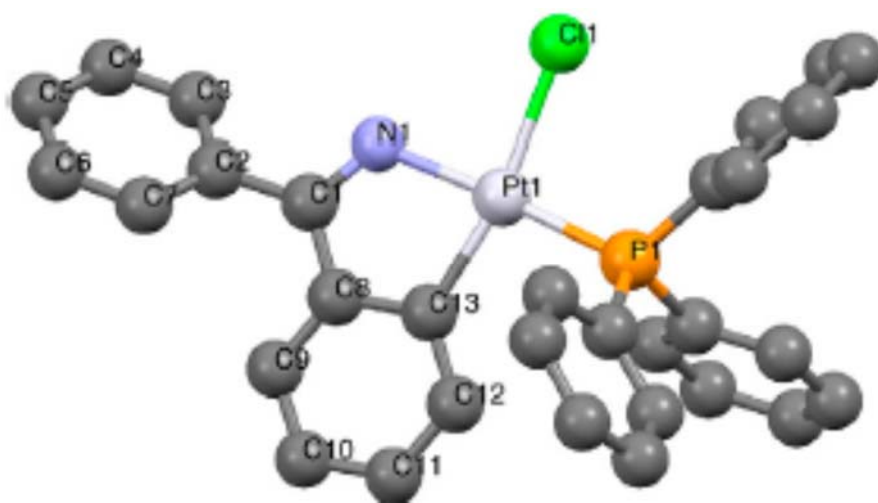
692

693

Figure 1

694

695



696

697

698

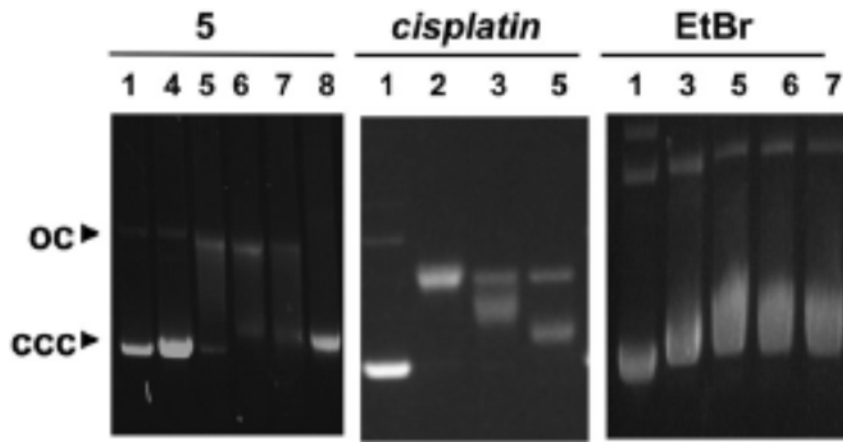
699

700

701

702
703
704

Figure 2



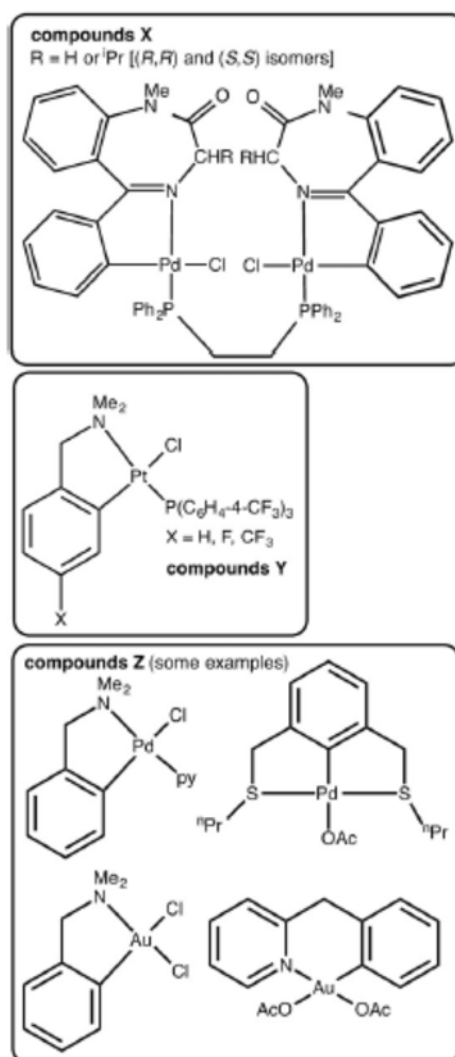
705
706
707
708
709

710

Figure 3

711

712



713

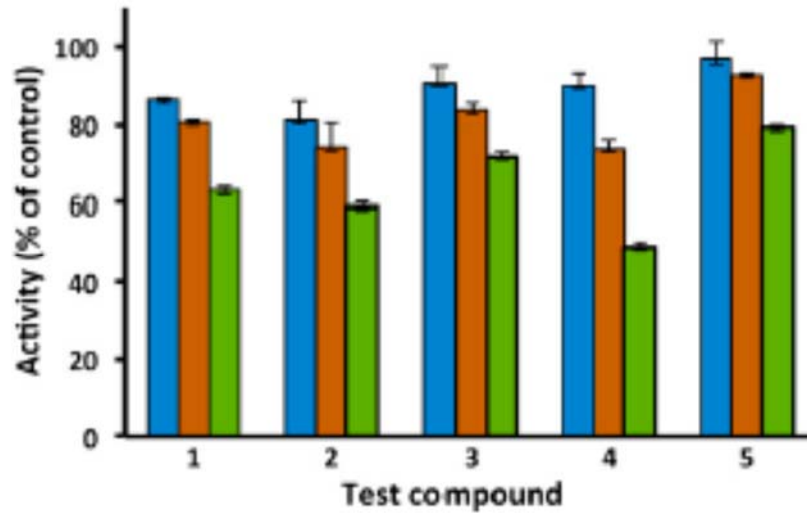
714

715

716

717
718
719

Figure 4



720
721
722
723